Versatile High Repetition Rate 2-μm Pulsed Source Based on Wideband Parametric Conversion

Adrien Billat, Steevy Cordette, *Member, IEEE*, and Camille-Sophie Brès, *Member, IEEE*

***Abstract*—We report an all-fiber pulsed source based on parametric conversion followed by thulium amplification able to deliver picosecond pulses at a repetition rate selectable between 2 and 5 GHz, of which central wavelength can be freely selected in the 2-μm region. A very versatile Nyquist pulse shaping of the parametric pump, which allows for the electrical control of the pulse train, enables such a freedom in the repetition rate selection, as well as some control in the pulse duration. We also show that data can be embedded in the output pulse train resulting in a high-quality Gb/s return-to-zero transmitter. Such a programmable short-wave infrared laser is of high interest for sensing or nonlinear optics applications around 2000 nm that require a fine adjustment in both the spectral and temporal domains.**

***Index Terms*—Doped fiber amplifiers, fiber lasers, fiber nonlinear optics, optical pulse generation, optical wavelength conversion.**

I. Introduction

PULSED lasers operating in the 2 μm spectral region are now widely used in various applications, ranging from transparent plastic material processing, laser lithotripsy or tissue ablation [1], remote sensing and lidars [2], advanced communication research [3], or for driving nonlinear light generation deeper in the mid-IR, where sub-ns pulse durations and high peak powers are required [4], [5]. Compelled by these demands, substantial progress has recently been made in thulium-doped and holmium-doped lasers and amplifiers. Nonetheless even if modelocked thulium-doped fiber (TDF) lasers are the widespread solution to address these needs, their cavity length generally prevents output repetition rates to be higher than a few tens of megahertz. For a subset of applications, a higher and programmable repetition rate is of interest. Being able to choose the duty cycle of the source would allow for the control of the pulse peak power, a particularly attractive feature for driving cascaded nonlinear effects towards the mid–IR. A high repetition rate cavity less pulsed source could also be combined with modulation capability for 2 μm communication. In addition, modelocked TDF laser cavities generally do not contain any optical filtering element such that the laser wavelength is rarely tunable. A wavelength tunable modelocked 2 μm laser was demonstrated but with megahertz repetition rate [6]. The difficulty to tune the wavelength can be a significant limitation for absorption line spectroscopy or nonlinear optics experiments, where one must achieve phase matching in a dispersive medium. On the other hand bulk solid state thulium lasers do not reach the performances of fiber sources in terms of ruggedness, mechanical stability and ease of operation.

In this work we demonstrate an all-fiber 2 μm wavelength tunable high repetition ration rate pulsed source. The fiber laser design is based on parametric wavelength conversion using exclusively standard telecom components, apart from the gain media, a concept demonstrated a few years ago [7]. The core operating principle relies on the efficient light conversion from a highly reconfigurable telecom pulsed source toward the short-wave infrared (SWIR) [8]. The remainder of the paper is organized as follows. This operating principle and the source implementation are described in Section II. In Section III, the experimental characterization of the pulsed parametric converter and the tunable 2 μm pulsed source is presented. In addition, we also show that the source can be adapted as a 2 μm transmitter. Finally the conclusion and discussion are given in Section IV.

II. Principle and Experimental Setup

A. Operating Principle

In the presented scheme, light generation around 2 μm is initiated by parametric conversion in a highly nonlinear fiber (HNLF). A tunable signal wave in the O-band (1250–1350 nm) interacts with an L-band pump via degenerate four-wave mixing (FWM) to give rise to an idler wave in the 1900–2100 nm range. For a pulsed pump wave, an idler wave with similar temporal characteristic is obtained; any reconfigurability features of the initial pulsed source are instantaneously copied onto the idler. However since such wideband FWM remains relatively inefficient, mainly due to dispersion fluctuations along the fiber, the average power obtained in the SWIR after the HNLF is generally low, even in pulsed pumping regime [2]. To overcome such limitation we previously suggested directly inserting a segment of TDF after the parametric converter [8]. The effect is twofold; first the TDF acts as a filter such that the O-band signal and L-band pump are absorbed by the Tm^{3+} ions, advantageously removing this undesired high power pump wave at the output of the source; second, the de-excitation of the $^3F_4$—$^3H_6$ transition strongly amplifies the idler located in the 2 μm region [9]. The schematic principle is plotted in Fig. 1.

In our previous work on thulium-assisted parametric conversion, all interacting waves were continuous, yielding a continuous-wave (CW) idler reaching a power of more than 700 mW over a wide wavelength range. An advantage of such a cavity-less generation scheme is that any modulation format

Manuscript received August 26, 2015; revised November 16, 2015; accepted November 20, 2015. Date of publication November 23, 2015; date of current version February 5, 2016. This work was supported by the European Research Council under Grant ERC-2012-StG 306630-MATISSE.

The authors are with the Photonic Systems Laboratory, Institute of Electrical Engineering, Ecole Polytechnique Federale de Lausanne, Lausanne 1015, Switzerland (e-mail: adrien.billat@epfl.ch; steevy.cordette@epfl.ch; camille.bres@epfl.ch).

Color versions of one or more of the figures in this paper are available online at http://ieeexplore.ieee.org.

Digital Object Identifier 10.1109/JLT.2015.2503602

0733-8724 © 2015 IEEE. Personal use is permitted, but republication/redistribution requires IEEE permission.
See http://www.ieee.org/publications_standards/publications/rights/index.html for more information.

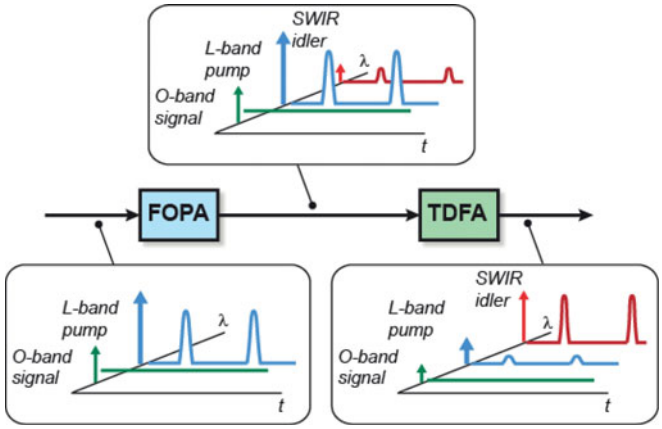

Fig. 1. Schematic of the pulsed idler generation and amplification in each stage. FOPA: fiber optical parametric amplifier, TDFA: thulium-doped fiber amplifier.

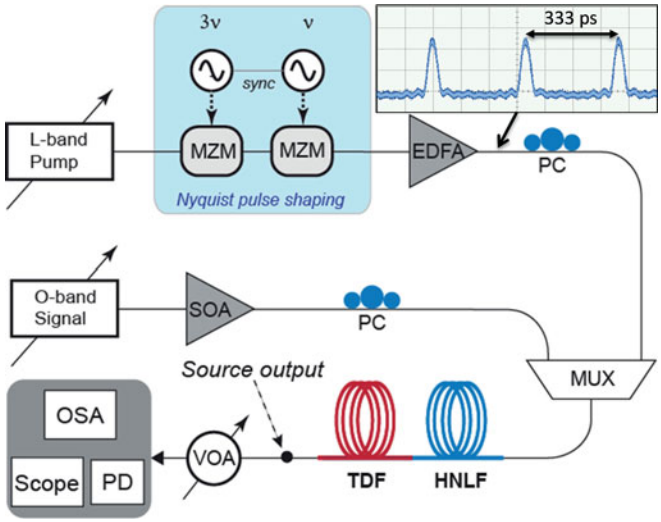

Fig. 2. Experimental setup. MZM: Mach–Zehnder modulator, SOA: semiconductor optical amplifier, PC: polarization controller, EDFA: erbium-doped fiber amplifier, MUX: 1310–1550nm wavelength multiplexer, VOA: variable optical attenuator, OSA: optical spectrum analyzer, PD: 2 μm photodetector. Inset: Pump pulse waveform at the HNLF input (recorded with a 50 GHz detector) at a repetition rate of 3 GHz.

on the pump or on the signal can in theory be reproduced on the idler [10], [11]. In practice a combination of linear and nonlinear effects along the propagation (dispersion, walk-off, self-phase modulation (SPM)) prevent perfect replication, especially if the interaction waveguide is long and the pulse duration is short. An optimization of the mixing fiber is therefore required in order to accommodate a pulsed pump featuring a repetition rate in the gigahertz range with picosecond pulse duration coupled with a CW O-band signal. In order to obtain a versatile SWIR pulsed source in terms of central wavelength, repetition rate or pulse width the generation of the L-band seed must also be malleable in terms of repetition rate and pulse duration. Moreover, tunability of the pump central wavelength is an interesting feature since parametric conversion in a HNLF requires some fine adjustment around the zero-dispersion wavelength (ZDW) in order to reach the most efficient conversion to the desired frequency [12]. Finally it is advantageous to keep the pump spectrally narrow (transform limited in the best case) since the pump spectral width is transferred to the idler along the propagation following the energy conservation principle [13].

For all these reasons and given the targeted frequencies, the L–band pulse train is shaped using a cascaded intensity modulators architecture [14]. The basic method consists of processing a CW laser through two successive Mach–Zehnder modulators (MZM), one being driven at a frequency ν and the second one at a frequency 3ν. When a proper bias and radio-frequency (RF) power are applied to the modulators a rectangular frequency comb of nine lines spanning 9ν is synthesized. Provided that the two RF sources are synchronized, the rectangular spectrum corresponds temporally to a train of sinc-shaped pulses at a repetition rate of ν and peak-to-zero crossing of $1/9\nu$ seconds. Such method allows for the required flexibility: the repetition rate and the duty cycle can be modified easily by controlling the RF driving signals or by adding a third stage as will be discussed in Section IV. The wavelength can be adjusted to any wavelength within the operating range of the modulators. Last but not least, this method relies solely on standard RF and telecom components.

B. Experimental Setup

The experimental setup is sketched on Fig. 2. The pump is shaped as previously described. A tunable CW and narrow linewidth (100 kHz) external cavity laser is sent through the two intensity modulators before being amplified to an average power between 1 and 2.5 W. For this demonstration, the repetition rate could be tuned to $\nu = 2$, 3 or 5 GHz. The repetition rate can however be easily scales to higher values. The pulse train at 3 GHz is shown in the inset of Fig. 2. The amplified spontaneous emission (ASE) from the booster is not filtered before the HNLF and is recycled in the next stage to pump the TDF. The boosted pump is then coupled to an amplified tunable CW O-band laser (13 dBm) before being launched into the HNLF and the TDF.

For pulsed operation up to 5 GHz, the length of the HNLF was optimized at 30 m. The HNLF from Sumitomo Electric features a nonlinear coefficient $\gamma = 14$ W^{-1}·km^{-1}, an average ZDW of 1569.05 nm, a third order dispersion $\beta_3 = 4.6 \times 10^{-2}$ ps^3/km and a fourth order dispersion assumed negative in average. Dispersion fluctuations originating from geometrical and doping fluctuations along the waveguide have a large impact on the evaluation of these parameters and on the efficiency of FWM when the pump-idler detuning is of the order of 40 THz [15]–[18]. The behavior of this fiber is further analyzed in the next section. The HNLF is followed by a commercial TDF (OFS TmDF200) of either 11.5 or 17.5 m depending on the targeted output wavelength. An optical attenuator is positioned at the output of the source to control the power sent to the measurement instruments; an optical spectrum analyzer (OSA) and an extended InGaAs 2 μm photodiode having a 22 GHz bandwidth. The wavelength dependence of the attenuator is taken into account when power levels or power ratios are computed from the optical spectra. Additionally a thermal power

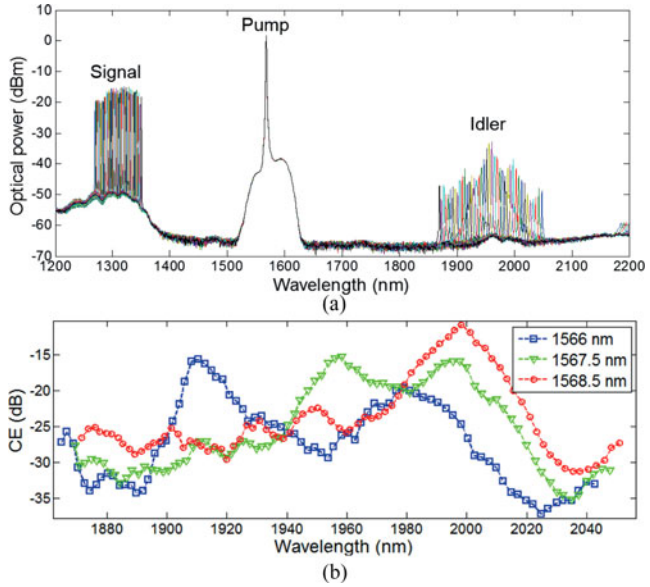

Fig. 3. (a) Superimposed FWM spectra after the HNLF for a pump wavelength of 1567.5 nm and a signal swept over the O-band (resolution 1 nm). (b) CE after the HNLF as a function of the idler wavelength and for the following pump wavelengths: 1566, 1567.5 and 1568.5 nm.

sensor is also used for absolute measurements after the HNLF or the TDF.

III. Results and Discussion

A. Parametric Converter Behavior

In order to optimize the overall performance of the 2 μm source, the parametric conversion in the HNLF is characterized. Due to phase matching considerations, slight adjustments to the pump wavelength are necessary in order to maximize the idler's intensity at any selected wavelength. Indeed even if the TDF stage can compensate for a low idler power at the HNLF output, the optical signal-to-noise ratio (OSNR) after Thulium amplification will be low if the TDF is not seeded with a sufficiently powerful idler. The protocol is the following: for each pump wavelength, the O-band signal is swept and the idler powers are recorded. The results were recorded for a 2 GHz repetition rate, a pump launch power of 1.7 W (in average) and are summarized in Fig. 3. Superimposed spectra for a 1567.5 nm pump are plotted in Fig. 3(a) while the conversion efficiency (CE) as a function of idler wavelength for three pump positions is shown in Fig. 3(b). The spectra are shown as they appeared on the OSA after the attenuator. The CE is computed as the ratio between the idler "effective power" (pulse energy over pulse duration) and the signal average power, both at the output of the HNLF, taking the wavelength-dependent attenuation function of the attenuator into account. The approximation is valid since the low efficiency of the FWM process yields a negligible change in the signal power. As expected the CE spectral peak evolves with the pumping wavelength, but the spectra also features multiple peaks shifting without apparent correlation, contrarily to what happens in a dispersion stabilized fiber [19]. In first approximation the multi-peaks effect of the CE can be ascribed to

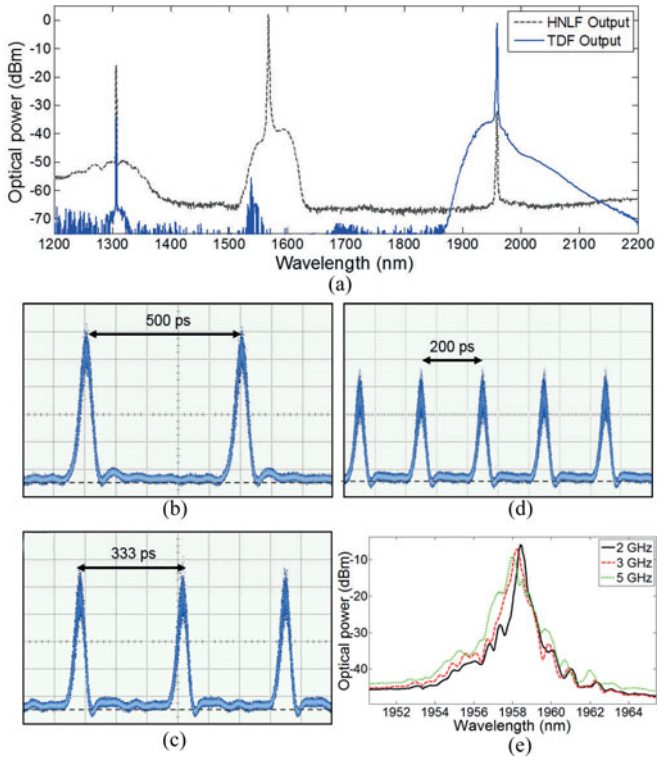

Fig. 4. (a) Spectra at the output of the HNLF and TDF for the 1958 nm idler configuration (resolution 1 nm). Pulse train recorded at the output of the source for a repetition rate of (b) 2 GHz, (c) 3 GHz and (d) 5 GHz. The dashed lines show the 0 V level. (e) Spectra of the idler at various repetition rate (resolution 0.1 nm).

dispersion variations along the waveguide having a long correlation length whereas the peaks broadening is attributed to the short-correlation length fluctuations. This effect is however hard to model and we limited ourselves to an empirical analysis in order to determine which pumping wavelength is optimal when targeting a given output wavelength for the laser. Two cases are studied in this article: the SWIR output around 1958 nm (pump at 1567.5 nm) and the SWIR output around 2001 nm (pump at 1568.5 nm). As it can be seen on Fig. 3(b), these configurations should yield optimized idler powers after the HNLF.

B. Overall Source Behavior

For the characterization of the source at a 1958 nm central wavelength, an 11.5 m TDF is appended at the HNLF output. The use of a relatively long doped fiber is necessary to redshift the peak of the gain spectrum toward 1958 nm and avoid detrimental effects such as spontaneous lasing [17] or OSNR degradation due to ASE. Spectra and pulse waveforms recorded right after the TDF are shown on Fig. 4. The spectra before and after the TDF for a 2 GHz repetition rate and a 1.7 W of pump power (at the HNLF input) are plotted in Fig. 4(a). The 1958 nm idler undergoes an amplification of 30 dB through the TDF while the L-band pump is entirely absorbed and the signal at 1310 nm strongly attenuated (20 dB). No filter is used after the TDF to remove ASE or to select the wavelength. Adjustment of the emission peak and proper idler seed power are sufficient to

guarantee a good OSNR (33 dB considering the peak to pedestal amplitude) at the desired wavelength after the amplifier.

The average power in SWIR at the source output in this configuration is measured to be 160 mW, independently of repetition rate. The waveforms at 2, 3 and 5 GHz repetition rate as seen in Fig. 4(b)–(d), respectively, indicate the generation of clean pulse trains, even in the absence of ASE filtering device before the detector. From the oscilloscope, the pulse duration in the three cases is 45, 36 and 33 ps. However, except for the 2 GHz case, the pulse bandwidth exceeds the one of the photodiode (as specified by the manufacturer) such that the value for higher speeds is likely to be limited by the photodiode impulse response. For the 2 GHz case, given the pulse duration, a pulse peak power of approximately 620 mW is retrieved. This value is expected to be similar in all three cases as the initial duty cycle is identical. Finally the idler spectra at the three rates are shown in Fig. 4(e) with, as expected, a slight broadening when ν is increased and consequently when the pump pulses are shortened. We ascribed this broadening to the SPM undergone by the pump, which becomes more pronounced as the pulse rise time is reduced. The spectral broadening is then transferred to the idler during its generation, as discussed in Section II. Cross-phase modulation, which exhibits a similar physics, is also likely to play a role here. Nonetheless, we believe that the idler is not powerful enough to be directly broadened by SPM through the HNLF, although it may happen in the TDF stage afterward [20].

Similar characterization was performed for the generation of a 2001 nm idler. In this configuration the pump was positioned at 1568.5 nm and a longer piece of TDF was used to further redshift the peak of the Thulium gain. In this case however, as the pumping power is limited by the previous stage and as the Tm^{3+} ions feature some absorption at 2 μm when they are not excited, a tradeoff must be found. A length of 17.5 m was selected as the best compromise in spite of the presence of a slight spontaneous lasing around 1919 nm (see Fig. 4(a)). It should be noted that even if the CE peaks at -11 dB in this configuration (see Fig. 3(c)), the O-band semiconductor amplifier is quite weak at the corresponding signal wavelength (1290 nm), and the subsequent idler absolute power drop leads to a less effective seeding of the TDF stage. We measure a 9 dB difference between the idler generated at 1958 nm and the 2001 nm one. Despite the still 30 dB amplification, the OSNR is therefore slightly degraded, translating to the addition of noise on the pulse train when the modulation speed is increased as can be seen in Fig. 5(b)–(d), in contrast with the previous results. This effect is further magnified due to the cutoff-frequency of the detector and leads to a poor waveform at 5 GHz. While a stronger signal source or a SWIR filter would be the most straightforward solutions, a dual-stage, long-wave amplification architecture would also help suppressing the ASE peak at 1950 nm [8], [21]. Finally, in such configuration the output average power is measured to be 37 mW, for a pulse peak power of approximately 142 mW at 2 GHz, while the idler spectra show a similar behavior as to the 1958 nm case (see Fig. 5(e)).

In both cases presented, the CE curves shown on Fig. 3(c) demonstrate that the pulse central wavelength can be tuned over several nm around the peak values located at 1960 and 2000 nm,

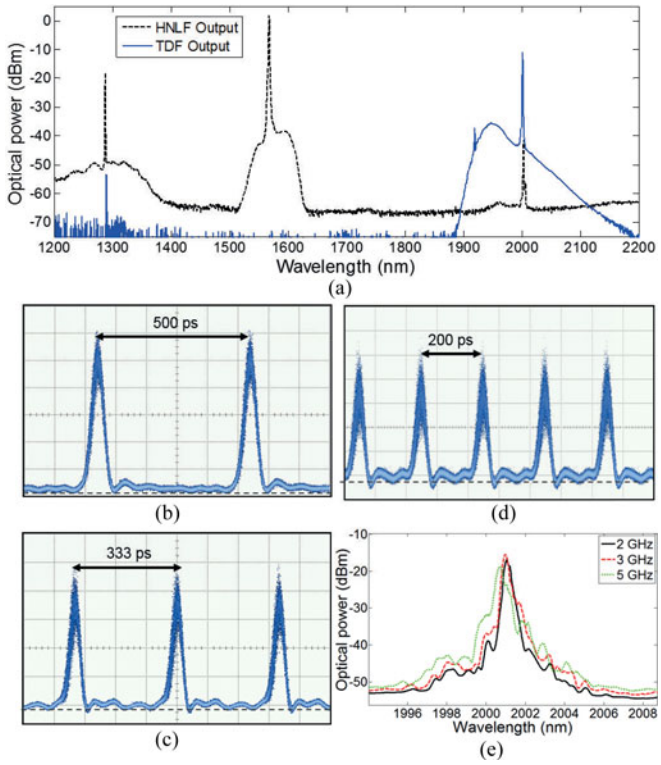

Fig 5. (a) Spectra at the output of the HNLF and TDF for the 2001 nm idler configuration (resolution 1 nm). Pulse train recorded at the output of the source for a repetition rate of (b) 2 GHz, (c) 3 GHz and (d) 5 GHz. The dashed lines show the 0 V level. (e) Spectra of the idler at various repetition rate (resolution 0.1 nm).

only by sweeping the O-band signal wavelength. For a larger SWIR wavelength change, the pump and the TDF amplifier have to be reconfigured as well. Overall the CE curves suggest that the source could operate between 1900 and 2000 nm seamlessly.

C. Data Transmission in SWIR

As previously mentioned an advantage of such cavity-less pulsed source is the possibility to easily modify the architecture to operate as a data transmitter. To strengthen this claim, we conducted an experiment to generate wavelength tunable high speed return-to-zero ON–OFF keying (RZ-OOK) data streams in the SWIR band. The OOK modulation is added on the pump pulse train by inserting a data modulator driven by a 2^{31}–1 pseudo-random bit sequence after the pulse shaping. The experiment was conducted for 3 Gb/s data generation and for a pump set at 1967.5 nm. Other settings could have easily been implemented. To additionally verify the wavelength tunability of the source, the O-band signal is swept between 1297.5 and 1320 nm leading to the generation of a RZ-OOK modulated idler in the range 1929–1980 nm. Within this range, we recorded the output OSNR of the signal and the bit error rate (BER). The SWIR bit sequence received on the photodiode is analyzed by an error-detector. During the procedure, the idler spectral peak power is kept constant at the photodiode input for all wavelengths at about -7 dBm. The results are summarized in Fig. 6. The eye patterns observed on the oscilloscope for two of the wavelength, 1940 and 1979 nm, are shown in Fig. 6(a) and (b). Other

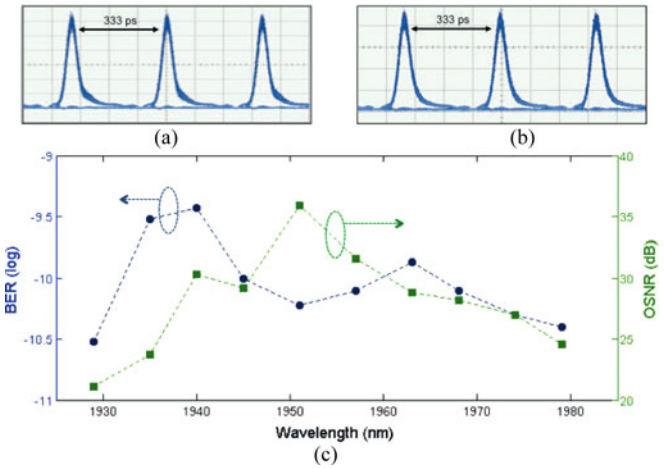

Fig. 6. Eye patterns of the modulated idlers at (a) 1940 nm and (b) 1979 nm. (c) BER (circles, left axis) and OSNR (squares, right axis) recorded for each tested wavelengths at a bit rate of 3 Gb/s.

wavelengths exhibited similar characteristics with a wide-open eye and a high extinction ratio. At such input power, the data conversion had a BER less than 10^{-9} over the whole tested wavelength range, in spite of some OSNR variations due to the variation in CE at the output of the HNLF. Even with the highest ASE level (such as at 1929 nm), the eye pattern is still wide open. As a simple observation, the noise appears to simply offset the entire waveform, adding a continuous component but leaving it clean for data carrying. It proves that a large degree of choice in the output wavelength is permitted without modifying the pump wavelength.

IV. Conclusion

In summary, we presented an all-fiber picosecond pulsed source capable of GHz repetition rate in the 2 μm band. It is based on FWM between a CW O-band signal, a pulsed L-band pump resulting in a pulsed SWIR idler. The latter is then amplified in a TDF pumped by the L-band wave in an energy efficient scheme relying only on standard telecom components. Thanks to the versatility of the Nyquist pulse carver, the repetition rate can be electrically controlled at will. A good replication of the original pulse train is maintained at a rate up to 5 GHz in the 1958 nm output configuration, with pulse duration of tens of picoseconds. We demonstrate the source operation around 1958 nm and 2001 nm. Even though the wavelength range accessible by sweeping only the signal is narrower than in previous experiments using a longer HNLF [22] due to the reduced amount of cumulated dispersion fluctuations, the entire range between 1900 and 2000 nm is accessible with a proper adjustment of the pump wavelength. For the source to operate at longer wavelengths (>2 μm), a powerful CW O–band laser and a long-band TDF amplifier configuration are necessary. The laser also proves able to output a RZ-OOK data sequence in SWIR as is shown at 3 Gb/s rate. This feature is necessary for SWIR free-space communications and could be used to realize a fast modulation of a lidar or spectrometer probing beam. To further improve the quality of the source for such applications it is possible to insert a bandpass filter at its output to remove the ASE.

Moreover, enhancements that can be easily implemented with the Nyquist pulse carver scheme theoretically allow for a decoupled control of the pulse duration and rep rate. On the one hand it has been shown that seeding one of the modulators with two or more properly selected RF tones allows for the densification of the rectangular frequency comb while preserving its linewidth [14]. This translates into reducing the pump repetition rate while keeping the same pulse duration and should impact the source output in the same way. On the other hand it is possible to keep the same spectral line spacing and broaden it with a third modulator or via FWM in a HNLF [23] before boosting it. This means that the pump pulse duration would be decreased at constant repetition rate. In both cases an augmentation of the pump peak will be obtained after the booster. As a result the CE should be increased through the HNLF, enabling the use of a shorter fiber. The main advantage of reducing the interacting length without sacrificing CE, is the possible increase of repetition rate (over 5 GHz) and/or decrease of the pulse duration (below 30 ps). As the nonlinear medium gets shorter, linear and nonlinear propagation phenomena's impact is reduced. In long waveguides and for picosecond pulses, SPM broadens dramatically the pump spectrum, preventing a good idler linewidth in SWIR. Additionally the high dispersion at 2 μm will chirp the generated pulses along the propagation whereas a group velocity mismatch between the L-band and the SWIR band will create a walk-off that broadens them during their generation. All these adverse effects are quenched when the fiber is kept short, potentially allowing increasing the repetition rate up to 10 GHz or more.

Acknowledgment

The authors would like to thank Sumitomo Electric Industries for providing the HNLF used in this study.

References

[1] J. Geng and S. Jiang, "Fiber lasers: The 2 μm market heats up," *Opt. Photon. News*, vol. 25, no. 7, pp. 34–41, Jul. 2014.

[2] S. Moro, A. Danicic, N. Alic, N. G. Usechak, and S. Radic, "Widely-tunable parametric short-wave infrared transmitter for CO2 trace detection," *Opt. Exp.*, vol. 19, no. 9, pp. 8173–8178, Apr. 2011.

[3] Z. Liu, Y. Chen; Z. Li, B. Kelly, R. Phelan, J. O'Carroll, T. Bradley, J. P. Wooler, N. V. Wheeler, A. M. Heidt, T. Richter, C. Schubert, M. Becker, F. Poletti, M. N. Petrovich, S.-U. Alam, D. J. Richardson, and R. Slavik, "High-capacity directly modulated optical transmitter for 2-μm spectral region," *J. Lightw. Technol.*, vol. 33, no. 7, pp. 1373–1379, Apr. 2015.

[4] M. Zhang, E. J. R. Kelleher, T. H. Runcorn, V. M. Mashinsky, O. I. Medvedkov, E. M. Dianov, D. Popa, S. Milana, T. Hasan, Z. Sun, F. Bonaccorso, Z. Jiang, E. Flahaut, B. H. Chapman, A. C. Ferrari, S. V. Popov, and J. R. Taylor, "Mid-infrared Raman-Soliton continuum pumped by a nanotube-mode-locked sub-picosecond Tm-doped MOPFA," *Opt. Exp.*, vol. 21, pp. 23261–23271, Sep. 2013.

[5] X. Liu, B. Kuyken, G. Roelkens, R. Baets, R. M. Osgood Jr, and W. M. J. Green, "Bridging the mid-infrared-to-telecom gap with silicon nanophotonic spectral translation," *Nature Photon.*, vol. 6, no. 10, pp. 667–671, Sep. 2012.

[6] Q. Fang, K. Kieu, and N. Peyghambarian, "An all-fiber 2-μm wavelength-tunable mode-locked laser," *IEEE Photon. Technol. Lett.*, vol. 22, no. 22, pp. 1656–1658, Nov. 2010.

[7] J. M. C. Boggio, S. Moro, B. P.-P. Kuo, N. Alic, B. Stossel, and S. Radic, "Tunable parametric all-fiber short-wavelength IR transmitter," *J. Lightw. Technol.*, vol. 28, no. 4, pp. 443–447, Feb. 2010.
[8] A. Billat, S. Cordette, Y.-P. Tseng, S. Kharitonov, and C.-S. Brès, "High-power parametric conversion from near-infrared to short-wave infrared," *Opt. Exp.*, vol. 22, no. 12, pp. 14341–14347, Jun. 2014.
[9] S. D. Agger and J. H. Povlsen, "Emission and absorption cross section of thulium doped silica fibers," *Opt. Exp.*, vol. 14, no. 1, pp. 50–57, Jan. 2006.
[10] F. Gholami, S. Zlatanovic, E. Myslivets, S. Moro, B. P.-P. Kuo, C.-S. Brès, A. O. J. Wiberg, N. Alic, and S. Radic, "10Gbps parametric short-wave infrared transmitter," presented at the Optical Fiber Communication Conf., Los Angeles, CA, USA, 2011, Paper OThC6.
[11] F. Gholami, B. P.-P. Kuo, S. Zlatanovic, N. Alic, and S. Radic, "Phase-preserving parametric wavelength conversion to SWIR band in highly nonlinear dispersion stabilized fiber," *Opt. Exp.*, vol. 21, no. 9, pp. 11415–11424, May 2013.
[12] B. P.-P. Kuo, N. Alic, P. F. Wysocki, and S. Radic, "Simultaneous wavelength-swept generation in NIR and SWIR bands over combined 329-nm band using swept-pump fiber optical parametric oscillator," *J. Lightw. Technol.*, vol. 29, no. 4, pp. 410–416, Feb. 2011.
[13] H. Min-Chen, M. E. Marhic, K. Y. K. Wong, and L. G. Kazovsky, "Narrow-linewidth idler generation in fiber four-wave mixing and parametric amplification by dithering two pumps in opposition of phase," *J. Lightw. Technol.*, vol. 20, no. 3, pp. 469–476, Mar. 2002.
[14] M. A. Soto, M. Alem, M. A. Shoaie, A. Vedadi, C.-S. Brès, L. Thévenaz, and T. Schneider, "Optical sinc-shaped Nyquist pulses of exceptional quality," *Nature Commun.*, vol. 4, no. 298, pp. 2–11, Dec. 2013.
[15] M. Farahmand and M. De Sterke, "Parametric amplification in presence of dispersion fluctuations," *Opt. Exp.*, vol. 12, no. 1, pp. 136–142, Dec. 2003.
[16] J. M. C. Boggio and H. L. Fragnito, "Simple four-wave-mixing-based method for measuring the ratio between the third- and fourth-order dispersion in optical fibers," *J. Opt. Soc. Am. B*, vol. 24, no. 9, pp. 2046–2053, Sep. 2007.
[17] A. Billat, S. Cordette, and C.-S. Brès, "Broadly tunable source around 2050 nm based on wideband parametric conversion and thulium–holmium amplification cascade," *Opt. Exp.*, vol. 22, no. 22, pp. 26635–26641, Oct. 2014.
[18] J. S. Y. Chen, S. G. Murdoch, R. Leonhardt, and J. D. Harvey, "Effect of dispersion fluctuations on widely tunable optical parametric amplification in photonic crystal fibers," *Opt. Exp.*, vol. 14, no. 20, pp. 9491–9501, Oct. 2006.
[19] B. P.-P. Kuo, M. Hirano, and S. Radic, "Continuous-wave, short-wavelength infrared mixer using dispersion-stabilized highly-nonlinear fiber," *Opt. Exp.*, vol. 20, no. 16, pp. 18422–18431, Jul. 2012.
[20] S. Kharitonov, A. Billat, L. Zulliger, S. Cordette, A. Vedadi, and C.-S. Brès, "Kerr nonlinearity of Thulium-doped fiber near 2 μm," presented at the Conf. Laser Electro-Optics, San Jose, CA, USA, 2015, Paper JTu5A.31.
[21] Z. Li, A. M. Heidt, J. M. O. Daniel, Y. Jung, S. U. Alam, and D. J. Richardson, "Thulium-doped fiber amplifier for optical communications at 2 μm," *Opt. Exp.*, vol. 21, no. 8, pp. 9289–9297, Apr. 2013.
[22] A. Billat, S. Cordette, and C.-S. Brès, "2 microns all-fiber picosecond pulse source with gigahertz repetition rate," presented at the Conf. Lasers Electro-Optics/ European Quantum Electron. Conf., Munich, Germany, 2015, Paper CD-1.6.
[23] S. Cordette, A. Vedadi, M. A. Shoaie, and C.-S. Brès, "Bandwidth and repetition rate programmable Nyquist sinc-shaped pulse train source based on intensity modulators and four-wave mixing," *Opt. Lett.*, vol. 39, no. 23, pp. 6668–6671, Dec. 2014.

Adrien Billat was born in Grenoble, France, in 1989. He received the Diplôme d'Ingénieur from the Ecole Supérieure d'Electricité, Paris, France, and the M.Sc. degree from the Ecole Polytechnique Fédérale de Lausanne (EPFL), Lausanne, Switzerland, both in 2013 and in electrical engineering. He is currently working toward the Ph.D. degree in electrical engineering at EPFL.

His current research interests include broadband fiber optical parametric converters, thulium-doped fiber lasers, and amplifiers and silicon-based nonlinear photonics.

Steevy Cordette (S'06–M'10) received the M.Sc. degrees in electrical engineering from the Higher School of Electrical Engineering, Rouen, France, and in electromagnetism and optoelectronics from the National Higher School of Aeronautics and Space, Toulouse, France, in 2006, and the Ph.D. degree in electrical engineering from the National Higher School of Telecom, Paris, France, in 2010.

He was a Consultant with the Telecom industry for two years. He joined the Photonic Systems Laboratory at the Ecole Polytechnique Fédérale de Lausanne, Lausanne, Switzerland, as a Research Scientist. His main research interests include nonlinear optical phenomena, all-optical signal processing, light generation, and optical communications.

Dr. Cordette has published more than 20 scientific papers in journals and international conferences, and holds three patents.

Camille-Sophie Brès (S'02–M'07) received the B.Eng. (Hons.) degree in electrical engineering from McGill University, Montreal, QC, Canada, in 2002, and the Ph.D. degree from Princeton University, Princeton, NJ, USA, in 2007. She is an Assistant Professor at Ecole Polytechnique Fédérale de Lausanne (EPFL), Lausanne, Switzerland. Prior to joining EPFL in 2011, she was a Research Scientist with the University of California, San Diego, CA, USA. Her research interests include all-optical signal processing based on nonlinear effects waveguides, mid-IR light generation, and optical communications. She has published more than 100 articles in peer-reviewed journals and international conferences. She currently serves on the technical program of the Optical Fiber Communication Conference and the European Conference on Optical Communication committees. She received an ERC Starting Grant in 2012 and the European Optical Society LIGHT2015 Young Women in Photonics Special Recognition Award.